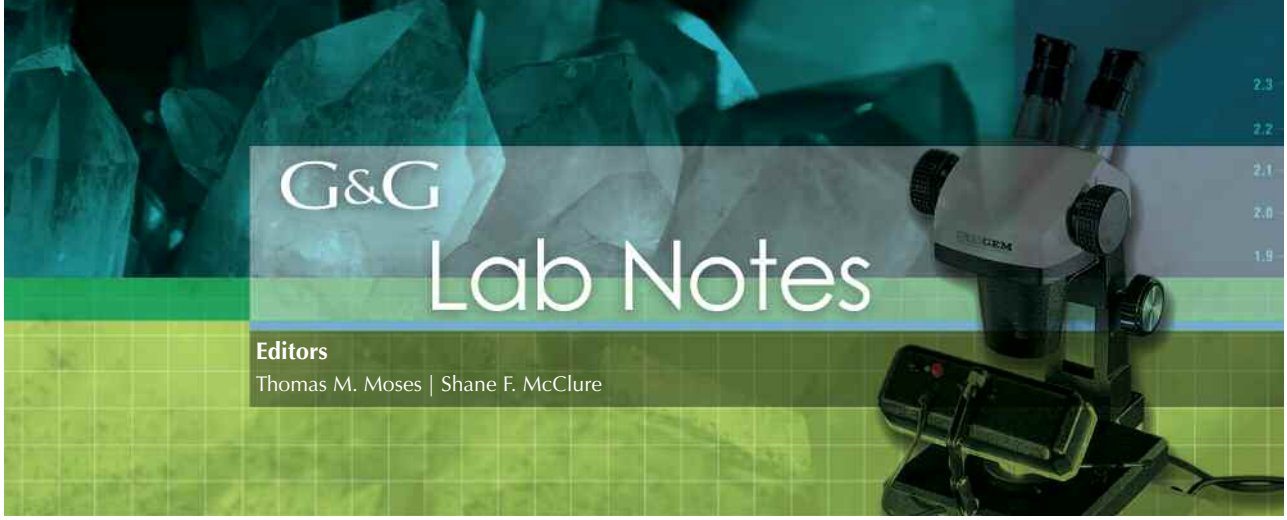

Cat's-Eye ALEXANDRITE with Unique Inclusion Pattern

Chatoyancy is an optical effect caused by light reflecting off dense concentrations of parallel needles or hollow tubes in cabochon-cut gem materials. To maximize chatoyancy, the base of the cabochon should be cut parallel to the inclusions to produce an even effect across the dome. In some cases, the parallel inclusions are not distributed throughout the stone and are only in zones or narrow bands. In such cases the cutter must orient the needles with care to produce a cat's-eye.

A chatoyant cabochon, weighing 21.22 ct and measuring 17.75 × 17.50 × 6.77 mm, was recently submitted to GIA's Tokyo laboratory for identification service. This stone displayed a change of color (figure 1) from brownish green in fluorescent light to brownish purple in incandescent light. Standard gemological testing resulted in a spot refractive index (RI) reading of 1.75, a specific gravity (SG) of 3.74, and strong trichroism. In addition to these properties, heterogeneous needle-like inclusions and infrared and Raman spectroscopy revealed that the stone was natural chrysoberyl.

What is notable about this stone is that all the needle-like inclusions that cause the chatoyancy are confined to a narrow layer at the very bottom of the cabochon (figure 2). The rest of the stone is nearly free of inclusions. The cutter obviously knew to orient what must have been a narrow layer of needles at the bottom of the cabochon so that the dome would form a complete cat's-eye. Some synthetic or imitation stones have an engraved foil backing or an engraved base to produce a cat's-eye or star in much the same way. Raman spectroscopic analysis indicated that the needle-like inclusions were rutile (figure 3). While the boundary between the included and

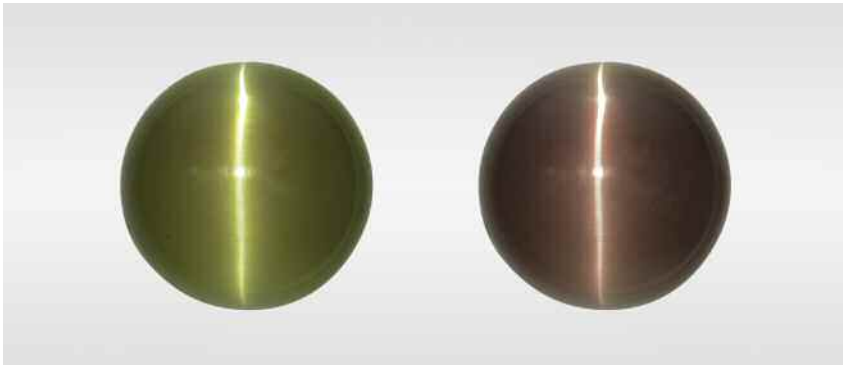

Figure 1. This alexandrite cabochon appears brownish green in fluorescent light (left) and brownish purple in incandescent light (right). The cabochon shows chatoyancy under both forms of illumination due to light reflection from the shallow plane of dense fine parallel needles.

Figure 2. A side view of the cabochon, immersed in water, showing the localized inclusions near the base. Field of view 1.6 cm.

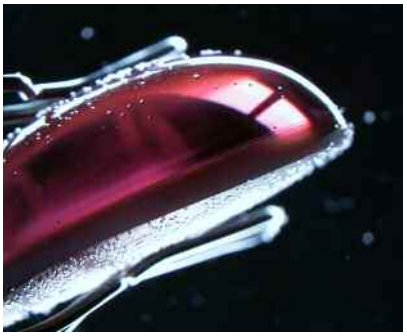

Figure 3. Iridescent minute parallel needles and particles in the alexandrite cabochon. Field of view 2.0 mm.

Editors' note: All items were written by staff members of GIA laboratories.

Gems & Gemology, Vol. 53, No. 4, pp. 459–464.

Figure 4. A 2.67 ct oval-cut diamond with uneven "lizard skin" surface texture. Close-up views of the pavilion with reflected light show how the textured pattern continues across facet junctions. Fields of view 3.56 mm (center) and 1.29 mm (right).

inclusion-free areas looks sharp, the stone is not assembled.

Makoto Miura and Yusuke Katsurada

Lizard Skin on Deformed DIAMOND

Facets that are nearly parallel to a diamond's octahedral crystal plane often develop a wavy, rippled appearance called "lizard skin" during polishing (e.g., J.I. Koivula, *The MicroWorld of Diamonds*, Gemworld International, Northbrook, Illinois, 2000, p. 63). The term is also used more broadly to describe any bumpy, uneven surface texture that develops on polished diamond facets. It is often attributed to polishing off-grain. Recently, GIA's New York lab encountered a 2.67 ct type IIa diamond (figure 4, left) with especially prominent lizard skin texture on multiple facets (figure 4, center and right). In this case, the texture appears to have developed due to a preexisting deformation fabric or structure inherent to the diamond itself, rather than merely as a consequence of poor polishing technique.

The surface texture has a pattern to it, with small bumps appearing to line up in corridors. Some corridors clearly continue from one facet to the next (figure 4, right). The continuity across facets suggests that this texture is the surface expression of irregularities that actually extend into the volume of the diamond itself. At high magnification with crossed polarizing filters, the lizard skin can be seen to conform to the shape and texture of the strain pattern within the diamond—that is, the pattern of bumps and depressions matches up where the intricate internal dark/light pattern of tatami birefringence meets the polished surface. This connection supports the idea that the surface texture is a reflection of underlying crystal imperfections.

Unusual hydrogen- and methane-bearing metallic inclusions in this diamond suggest it originated from extreme depths of about 360–750 km in the earth's mantle (E.M. Smith et al., "Large gem diamonds from metallic liquid in Earth's deep mantle," *Science*, Vol. 354, No. 6318, 2016, pp. 1403–1405). In this high-temperature environment, deformation and annealing over a long period of time may have given the diamond a mosaic crystal structure. This natural phenomenon occurs when heat allows the crystal to undergo recovery, a process of dislocation reorganization that divides the distorted grain into a mosaic of smaller, undistorted subgrains without new crystal growth. The subgrains, measuring about 10–30 microns, are like bricks in a wall; while the wall may be slightly curved, the individual bricks are not distorted. These distortions become localized as subgrain boundaries rather than spreading continuously through the crystal. As a result, the subgrains will be oriented in slightly different directions.

Because polishing is so strongly dependent on crystal orientation, if a single facet consists of a mosaic of subgrains with varying orientation, polishing will be uneven. The resulting surface may develop a pattern of bumps and depressions that mimics the size and shape of underlying subgrains and, in turn, reflects the diamond's natural deformation history. Samples like this one are interesting for scientists because little is known about the geological conditions that lead to the various deformation-related features seen in natural diamonds.

Evan M. Smith and Paul Johnson

Gota de Aceite in a Zambian EMERALD

Gota de aceite (Spanish for "drop of oil"), a rare phenomenon that occurs in the finest emeralds, is typically associated with Colombian origin (R. Ringsrud, "*Gota de aceite*: Nomenclature for the finest Colombian emeralds," Fall 2008 *G&G*, pp. 242–245). The phenomenon creates a roiled effect caused by irregularity in the emerald's internal crystal structure. During the gemstone's crystallization the growth conditions are altered, giving rise to rapid columnar growth. When looking down the emerald's c-axis, the outline of the columns can be seen. This sometimes has the appearance of drops of oil, giving rise to the name. The columns typically have a slightly different trace element composition from that of the host emerald. This heterogeneity in trace element chemistry will cause a minor change in the refractive

index of the columns, allowing the structure to be visible.

The Carlsbad laboratory recently received a 2.10 ct emerald for origin determination. The stone had blocky multiphase inclusions and ilmenite scattered throughout, along with mica platelets and a very subtle blue flash effect associated with some small feathers. At a certain angle, a muted gota de aceite effect was also visible (figure 5). The UV-Vis spectrum shows a distinct Fe^{2+} broad band at approximately 900 nm. Inductively coupled plasma–mass spectrometry (ICP-MS) confirmed the stone's relatively high iron content and indicated a chemical composition consistent with Zambian origin.

The gota de aceite seen in this Zambian emerald was not exactly the same as the phenomenon found in Colombian emeralds. Dendritic ilmenite, an iron-rich mineral, was fully enclosed in the columnar structure. We believe the epigenetic ilmenite exsolved the increased iron content, as Zambian emeralds contain a larger amount of iron than their Colombian counterparts (J.C. Zwaan et al., "Emeralds from the Kafubu area, Zambia," Summer 2005 *G&G*, pp. 116–148).

Until now, gota de aceite has only been documented in Colombian emeralds and has been an aid in origin determination. Still, this is not the first time that an inclusion indicative of a particular origin has been found elsewhere. Jagged three-phase inclusions, traditionally seen in Colombian emeralds, have also been documented in emeralds from certain mines in Afghanistan, China, and Zambia (S. Saeseaw et al., "Three-phase inclusions in emerald and their impact on origin determination," Summer 2014 *G&G*, pp. 114–132). This emerald shows that inclusions may not always provide conclusive proof of origin, but they can still provide useful information.

Nicole Ahline

Figure 5. A muted gota de aceite *effect, with epigenetic ilmenite, in an emerald from Zambia. Field of view 1.26 mm.*

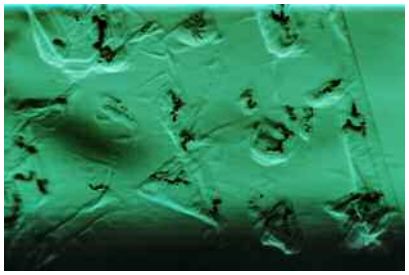

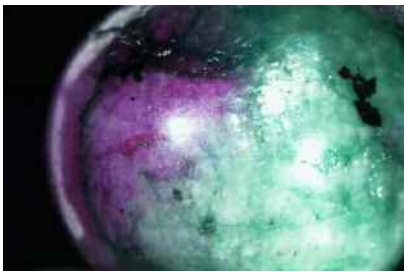

Figure 6. Green to dark green and pinkish purple to dark purple dye concentrations were observed in the fissures and structure of this quartzite, which resembled ruby-in-zoisite. Field of view 9.61 mm.

Dyed QUARTZITE Imitation of Ruby-in-Zoisite

The New York laboratory recently received a bracelet composed of translucent multicolored beads that closely resembled ruby-in-zoisite. Standard gemological testing of one of the round beads (measuring 8.33 × 8.17 mm) revealed an RI of 1.55 for both the purple and green areas (instead of approximately 1.76 or 1.69 for ruby and zoisite, respectively) and very weak red to inert fluorescence in long-wave and short-wave ultraviolet light, respectively. Microscopic observation revealed fissures and a translucent aggregated/grainy structure, both of which contained green to dark green and pinkish purple to dark purple dye concentrations (figure 6).

Although most of the translucent green and purple aggregate material we encounter for identification is ruby-in-zoisite, the gemological features of this bead were inconsistent with our expectations. Raman spectra were collected to confirm the identity. Spectra from both the purple and green areas matched quartz (figure 7). Since the material was an aggregate, we concluded that it was dyed quartzite.

The Lab Notes section has documented many cases of dyed quartzite

Figure 7. Raman spectra collected from the sample's purple and green areas indicated quartz rather than ruby and zoisite. Spectra are offset for clarity.

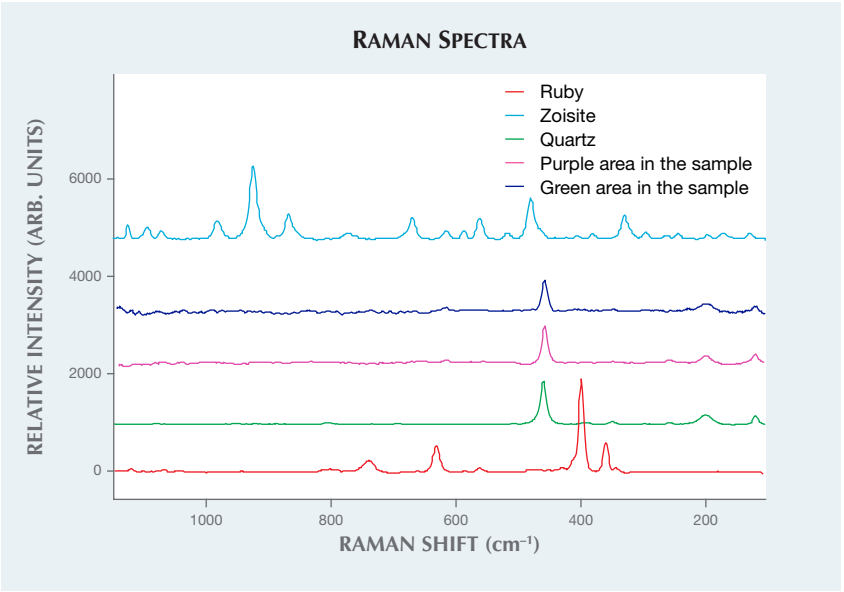

imitating jadeite, ruby, lapis lazuli, and sugilite (Spring 1986, pp. 49–50; Summer 1991, pp. 122–123; Summer 1995, pp. 125–126; Summer 1998, pp. 131–132; Spring 2001, pp. 62–63; and Fall 2003, pp. 219–220). But this is the first example we have seen of quartzite being used to imitate ruby-in-zoisite. This dyed quartzite provides an intriguing example for consumers to be aware of when purchasing ruby-in-zoisite.

HyeJin Jang-Green

SYNTHETIC MOISSANITE
Imitating Rough Diamond

The Carlsbad laboratory recently examined a very light green 9.71 ct specimen (figure 8), measuring 11.79 × 9.69 × 11.61 mm, that was submitted as a rough diamond. The sample resembled a diamond octahedron, with surface growth features and a bright vitreous to subadamantine luster. Closer examination of its habit and surface features, along with gemological and advanced testing results, revealed it to be a synthetic moissanite.

The specimen was not a true octahedron, as is typical of a diamond crystal, but a rectangular bipyramid with 10 faces (eight triangular and two hexagonal side pinacoids on the girdle). The surface was dimpled, and two of the faces had deep striations resembling growth features in a rough diamond. Irregularly shaped and sub-hexagonal etch pits (figure 9), along with some dark brown residue, were also found on the surface. Due to the uneven surface, observation of internal features was limited to some small scattered pinpoint inclusions and a few etch tubes (figure 10). The surface also made it difficult to see any doubling effect or a doubly refractive reaction in the polariscope. Viewed in plane-polarized light, however, a large twinning plane crossed the crystal diagonally, bluish green on one side and colorless on the other. This dichroism served as proof of the stone's doubly refractive nature, as opposed to singly refractive diamond. Standard gemological properties of the stone offered further evidence of its true identity, including an over-the-limit refractive index reading, a hydrostatic SG of 3.23, very weak yellow fluorescence in both long-wave and short-wave UV, and a uniaxial optic figure. These properties and advanced testing results, including Fourier-transform infrared (FTIR) and Raman spectrometry, identified the specimen as synthetic moissanite. It is important to note that although natural moissanite exists, it is extremely rare and gem-quality material has never been found. Natural moissanite commonly occurs in fragmented pieces and in much smaller sizes (the largest known specimen measured 4.1 mm), often with a creamy white or red matrix (Summer 2014 GNI, pp. 160–161). That was not the case for this 9.71 ct synthetic moissanite.

Gemological and advanced testing are indispensable tools for revealing the true identity of gems, especially simulants and imitations with an appearance that can easily deceive the general public. While there is no evidence that this specimen was deliberately deceptive,

Figure 8. A very light green 9.71 ct synthetic moissanite crystal, submitted to the Carlsbad laboratory as a rough diamond. Field of view approximately 14 mm.

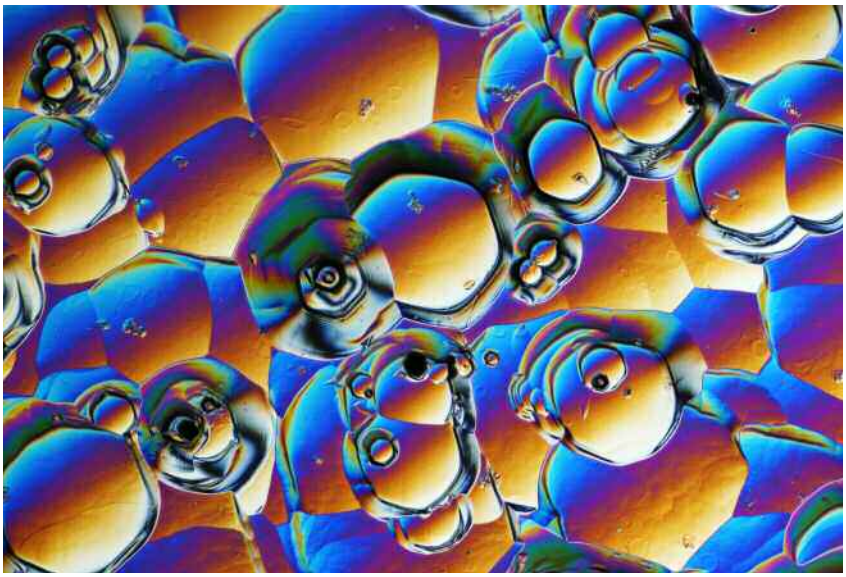

Figure 9. Sub-hexagonal etch pits in synthetic moissanite are observed using differential interference contrast. Field of view approximately 1.44 mm.

Figure 10. Etch tubes extended from surface etch pits and ended at the twinning plane. Field of view approximately 2.30 mm.

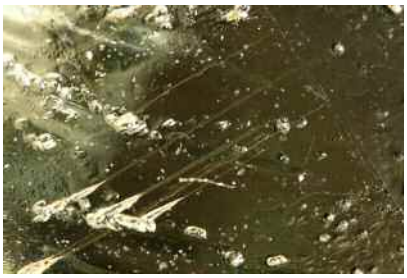

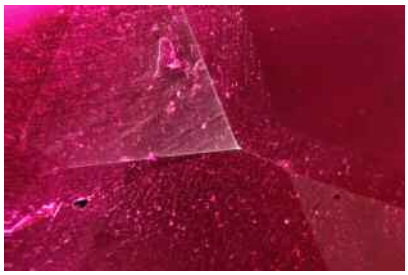

Figure 11. A thin layer of synthetic ruby overgrowth with flux particles is distinct from the natural sapphire seed visible in the upper right of the image. Field of view 1.99 mm.

TABLE 1. Trace elements in two synthetic ruby overgrowth samples, detected by LA-ICP-MS (avg. concentration in ppmw[a]).

Element	Concentration in overgrowth	Standard deviation
Cr	32,866	1342
Fe	1231	101.4
Ga	47.6	2.40
Mg	4.92	1.69
Mn	4.55	0.31
Mo	bdl[b]	—
Ni	34.9	49.5
Ti	19.06	6.94
Pt	4.03	4.07
Zr	0.41	0.71

[a] *Six spots examined in total.*
[b] *bdl: below detection limit. Detection limit was 0.013 ppmw for both samples.*

gemological knowledge is important in preventing accidental and intentional acts of fraud and preserving the integrity of the trade.

Rebecca Tsang

Two Unusual Natural Sapphires With SYNTHETIC RUBY Overgrowth

The New York laboratory recently received two loose red oval mixed cuts for identification. Standard gemological testing yielded refractive indices slightly higher than expected for corundum: 1.778–1.788 and 1.776–1.787, while a typical RI for corundum is 1.762–1.770. Elevated RIs for chromium-diffused corundum have been reported and may be attributed to higher Cr_2O_3 concentration at the surface (S.F. McClure et al., "Update on diffusion-treated corundum: Red and other colors," Spring 1993 *G&G*, pp. 16–28). To the unaided eye, the stones appeared to be chromium diffused, displaying red color concentration at the facet junctions, but their synthetic component became apparent upon further observation.

Microscopic examination revealed that planes of minute particles demarcated a thin layer, approximately 0.3 mm thick, of synthetic overgrowth from a natural sapphire core (figure 11). The presence of intact silk and heat-altered crystal inclusions confirmed the seeds to be natural (figure 12). A series of shallow flux-fingerprints cracking the surface suggested a flux growth process (figure 13). Portions of the near-colorless core could be seen in areas where the overgrowth was cut away during polishing (figure 14). These windows showed a sharp boundary without "bleeding" of the saturated red overgrowth into the near-colorless seed, which is typically observed in chromium-diffused corundum (McClure et al., 1993). The windows into the near-colorless seed also indicate that most or all of the red color is concentrated in the synthetic ruby overgrowth.

The overall appearance of the two stones was similar to the now-rare Lechleitner synthetic overgrowth

Figure 12. A fuzzy heat-altered crystal inclusion commonly referred to as a "snowball" is surrounded by a discoid fracture, proving the natural origin of the corundum seed. Field of view 1.26 mm.

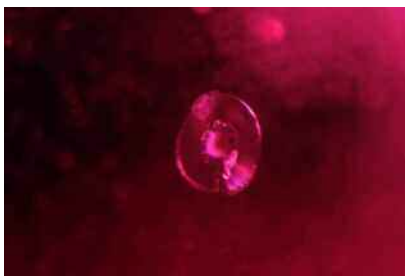

Figure 13. Reflective silk inclusions in the natural sapphire seed are visible behind a coarse flux fingerprint in the synthetic ruby overgrowth, which was cut through during the fashioning process. Field of view 3.57 mm.

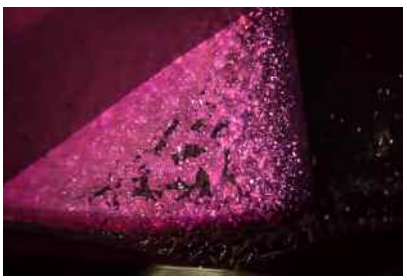

Figure 14. A portion of the near-colorless corundum seed is revealed in an area where the synthetic ruby overgrowth was cut away during fashioning. Field of view 10.85 mm.

Figure 15. A thin layer of synthetic emerald deposited on a near-colorless beryl seed, a type of synthetic emerald first marketed by Johann Lechleitner in the early 1960s. Field of view 3.57 mm.

emeralds, which are composed of a near-colorless beryl seed with synthetic emerald overgrowth. A sample with this type of synthetic emerald overgrowth was coincidentally submitted to the Carlsbad laboratory for identification around the same time (figure 15). In addition to emeralds, Lechleitner also experimented with ruby overgrowth on both synthetic and natural corundum seeds (K. Schmetzer and H. Bank, "Lechleitner synthetic rubies with natural seed and synthetic overgrowth," *Journal of Gemmology*, 1988, Vol. 21, No. 2, p. 95–101), with the most commonly documented versions containing synthetic seeds (E.J. Gübelin and J.I. Koivula*, Photoatlas of Inclusions in Gemstones,* Vol. 2, Opinio Verlag, Basel, Switzerland, 2005, p. 352; Fall 2014 Lab Notes, pp. 242–243).

Advanced testing on the synthetic ruby overgrowth layer using laser ablation–inductively coupled plasma–mass spectrometry (LA-ICP-MS) revealed the presence of Cr, Fe, Ga, Mn, Mg, Ni, Ti, Pt, and Zr (table 1). These results, specifically the presence of platinum, are consistent with previously reported synthetic ruby overgrowth (S. Saeseaw et al., "Analysis of synthetic ruby overgrowth on corundum," *GIA News from Research*, June 10, 2015). Molybdenum was reported in the primary examination of Lechleitner overgrowth rubies (Schmetzer and Bank, 1988), and its absence here suggests alternative growth conditions for these samples.

Although this is not the first report of synthetic ruby overgrowth on natural sapphire seeds (Schmetzer and Bank, 1988; C.P. Smith, "Diffusion ruby proves to be synthetic ruby overgrowth on natural corundum," Fall 2002 *G&G*, pp. 240–248), it marks the first time the New York and Carlsbad laboratories have had them submitted for identification. The resurfacing of these vintage overgrowth synthetics shows that once a material is in the trade, it is here to stay.

Tyler Smith and Hollie McBride

PHOTO CREDITS

1—Shunsuke Nagai; 2 and 3—Makoto Miura; 4—Evan Smith; 5—Nathan Renfro; 6—HyeJin Jang-Green; 8–10—Rebecca Tsang; 11–15—Hollie McBride.

THANK YOU, REVIEWERS

Gems & Gemology requires each manuscript submitted for publication to undergo a rigorous peer review process, in which a paper is evaluated by at least three experts in the field prior to acceptance. This is essential to the accuracy, integrity, and readability of *G&G* content. In addition to our dedicated Editorial Review Board, we extend many thanks to the following individuals who devoted their valuable time to reviewing manuscripts in 2017.

Non-Editorial Board Reviewers

Ilaria Adamo • Donald Burnett • Gagan Choudhary • Zachary Cole • Si and Ann Frazier • Dan Frost • Artitaya Homkrajae • Richard Hughes • Dorrit Jacob • John King • Maya Kopylova • Glenn Lehrer • Cigdem Lule • Carmel McDougall • Tetsuji Masaoka • Jana Miyahira-Smith • Lutz Nasdala • Laura Otter • Karl Schmetzer • Olivier Segura • Sherris Cottier Shank • Elena Shuchukina • Nicholas Sturman • Ziyin Sun • Rachelle Turnier • Chunhui Zhou

Cast Your Vote for the 2017 Dr. Edward J. Gübelin Most Valuable Article Award

Established in 1981, *G&G*'s Most Valuable Article Award invites the journal's readers to vote on the three most important articles (feature articles, field reports, and charts) from the previous year. Each completed ballot is entered into a drawing to win a one-year subscription to *Gems & Gemology*.

To qualify for the drawing, please submit your votes for the 2017 MVA Award by **Monday, March 12, 2018**, either by mail, by scanning the QR code, or by visiting www.gia.edu/most-valuable-article-2017